Supplementary information

Supplementary Table 1-2

Supplementary Table 1, Summary of antibodies used in this study

ID	Company	Cat	Clone number
SHP2	CST	3397S	D50F2
ERK	CST	4695	137F5
p-ERK	CST	4370	D13.14.4E
Vimentin	Abcam	Ab193555	EPR3776
α-SMA	Abcam	Ab32575	E184
Desmin	Abcam	Ab15200	Polyclonal
Ki-67	Abcam	Ab15580	Polyclonal
p-AKT	CST	4060	D9E
AKT	CST	2920	40D4
p-mTOR	Invitrogen	SB233656A	Polyclonal
mTOR	Invitrogen	PA5-34663	Polyclonal
HIF1α	Invitrogen	MA1-16504	H1alpha67
β-Actin	CST	3700	8H10D10
β-Tubulin	Invitrogen	32-2600	2 28 33
HSP60	Invitrogen	PA5-34760	Polyclonal
OXPHOS Rodent WB Antibody Cocktail	Thermo	45-8099	Cocktail
NDUFB8	Abcam	Ab251160	EPR15961
UQCRC2	Abcam	Ab240368	EPR13051
AMPK	CST	5831	D5A2
p-AMPK	CST	50081	D4D6D
S6	CST	2217	5G10
p-S6	CST	4858	D57.2.2E
ACC	CST	3662	Polyclonal
p-ACC	CST	3661	Ser79
IBA1	CST	17198	E4O4W
CD133	Invitrogen	PA5-38014	Polyclonal
CD133-APC	Biolegend	141208	315-2C11
Frizzled-1 Antibody, anti-mouse, PE	Miltenyi Biotec	130-112-397	REA603
CD271- Alexa Fluor™ 488	eBioscience	53-9400-42	ME20.4
CD184-PE	Biolegend	146505	L276F12
S100A4	Abcam	Ab218512	S100A4/1482
MyoD1	CST	13812	D8G3

Myogenin	Invitrogen	14-5643-80	F5D
Caldesmon	Thermo	PA5-27719	Polyclonal
S100-β	Abcam	Ab52642	EP1576Y
Sox9	Thermo	PA5-81966	Polyclonal
Aggrecan	Thermo	MA5-42646	6L4T2

Supplementary Table 2, Summary of primers used in this study

Primer ID	Sequence (5' to 3')
Neo-F	TACCTTGAGGTTAGTGAACGTCA
Neo-R	CGCTCTCGTTTTCCCCATAATC
β-actin-F	GGCTGTATTCCCCTCCATCG
β-actin-R	CCAGTTGGTAACAATGCCATGT
18s-F	TAGAGGGACAAGTGGCGTTC
18s-R	CGCTGAGCCAGTCAGTGT
CytB-F	CCACTCATTCATTGACCTACCT
CytB-R	GCTCCGTTTGCGTGTATATATC

Supplemental Figures 1-15

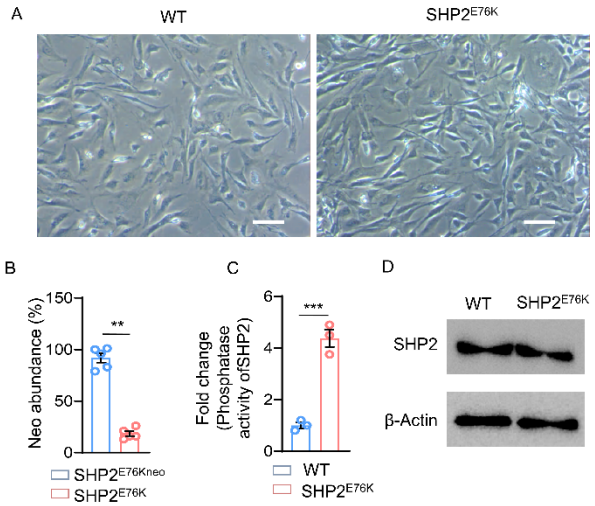

Supplemental Figure 1. Measurement of Mx1-cre-mediated recombination in WT and SHP2^{E76K} MSCs. **A** Representative image of WT and SHP2^{E76K} MSCs in culture. **B** Statistical analysis of neo abundance in MSCs expressing SHP2$^{E76K\text{-}neo}$ or SHP2^{E76K} (n=5 per group). Data are represented as the means ± SD. $^{**}p < 0.01$ (two-tailed unpaired t test). **C** Statistical analysis of SHP2 phosphatase activity in WT and SHP2^{E76K} MSCs (n=3 per group). Data are represented as the means ± SD. $^{***}p < 0.001$ (two-tailed unpaired t test). **D** Western blot analysis of SHP2 expression in Mx1-cre and Mx1-cre; SHP2^{E76K} mouse MSCs.

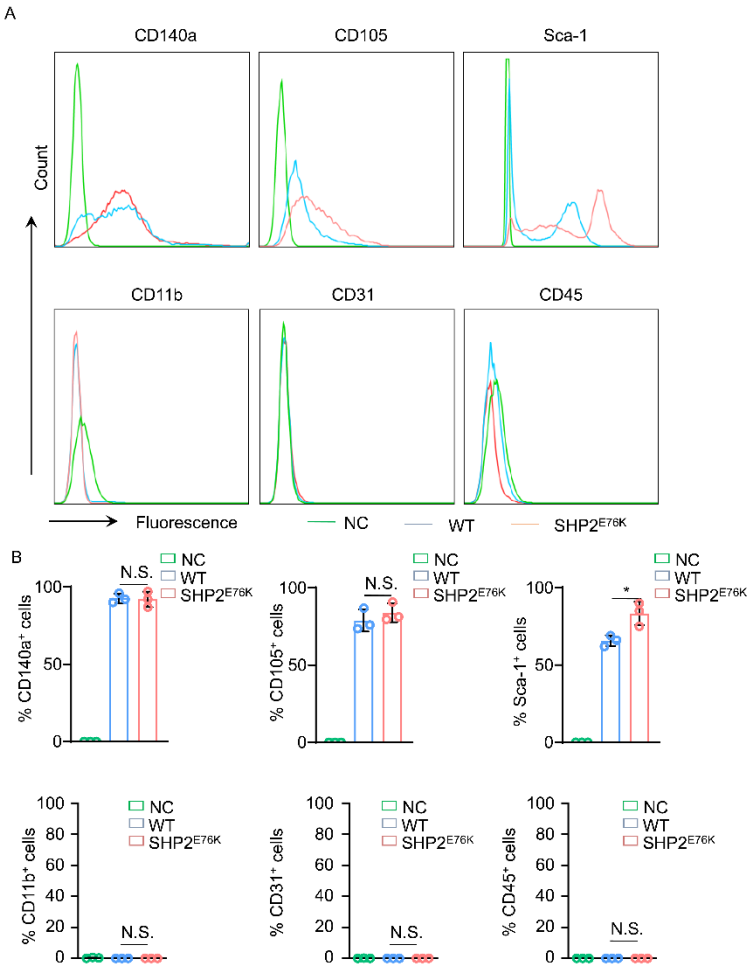

Supplemental Figure 2. Characterization of WT and SHP2^{E76K} MSCs. A Flow cytometry validation of MSCs using different markers, including CD140a, CD105, Sca1, CD11b, CD31 and CD45. **B** Statistical analysis of the population of CD140a^{+}, CD105^{+}, Sca1^{+}, CD11b^{+}, CD31^{+} or CD45^{+} cells among WT and SHP2^{E76K} MSCs (n=3 per group). Data are represented as the means ± SD. *$p < 0.05$, N.S. indicates no significance (two-tailed unpaired t test). indicates no significance (two-tailed unpaired t test).

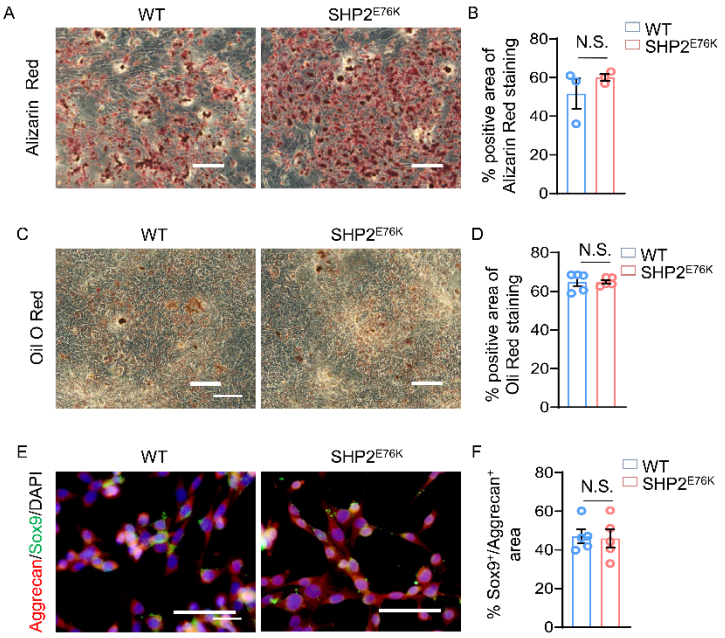

Supplemental Figure 3. There was no significant difference in trilineage differentiation capacity between WT and SHP2^{E76K} MSCs. A, B Representative images (**A**) and statistical analysis (**B**) of Alizarin Red staining in MSCs with or without GOF mutant SHP2 (n=3 per group). Data are represented as the means ± SD. N.S. indicates no significance (two-tailed unpaired t test). Scale bar, 200 μm. **C, D** Representative images (**C**) and statistical analysis of Oil Red O staining (**D**) in MSCs with or without GOF mutant SHP2 (n=5 per group). Data are represented as the means ± SD, N.S. indicates no significance (two-tailed unpaired t test). Scale bar, 100 μm. **E, F** Representative IF images (**E**) and statistical analysis (**F**) of the SOX9^{+}/Aggrecan^{+} area in MSCs with or without GOF mutant SHP2 (n=5 per group). Data are represented as the means ± SD, N.S. indicates no significance (two-tailed unpaired t test). Scale bar, 200 μm.

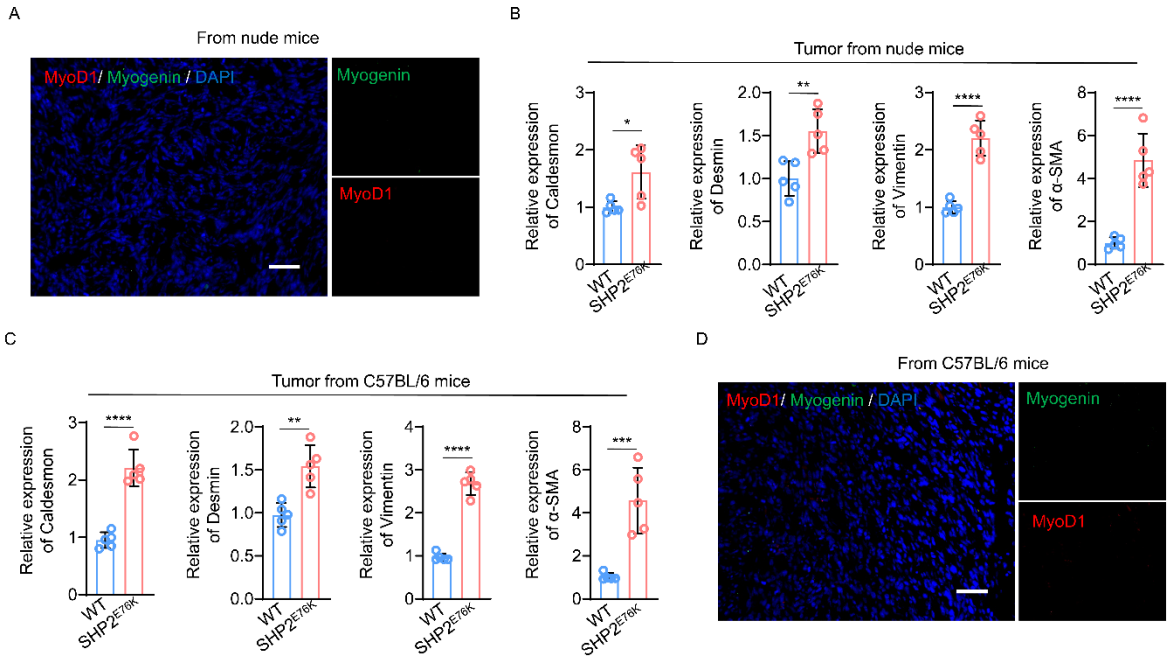

Supplemental Figure 4. SHP2^{E76K} MSC-initiated sarcomas did not express MyoD1 and Myogenin. A Representative immunofluorescence images of MyoD1 and Myogenin staining in sarcomas developed from nude mice. Scale bar, 100 μm. **B** Statistical analysis of Caldesmon, Desmin, Vimentin and α-SMA in normal subcutaneous tissue (with WT MSC injection) and sarcomas (with SHP2^{E76K} MSC injection) from nude mice (n=5 per group). Data are represented as the mean ± SD. *$p < 0.05$, **$p < 0.01$, ****$p < 0.0001$ (two–tailed unpaired *t* test). **C** Statistical analysis of Caldesmon, Desmin, Vimentin and α-SMA in normal subcutaneous tissues (with WT MSC injection) and sarcomas (with SHP2^{E76K} MSC injection) from C57BL/6 mice (n=5 per group). Data are represented as the mean ± SD. **$p < 0.01$, ***$p < 0.001$, ****$p < 0.0001$ (two–tailed unpaired *t* test). **D** Representative immunofluorescence images of MyoD1 and Myogenin staining in sarcomas developed from C57BL/6 mice. Scale bar, 100 μm.

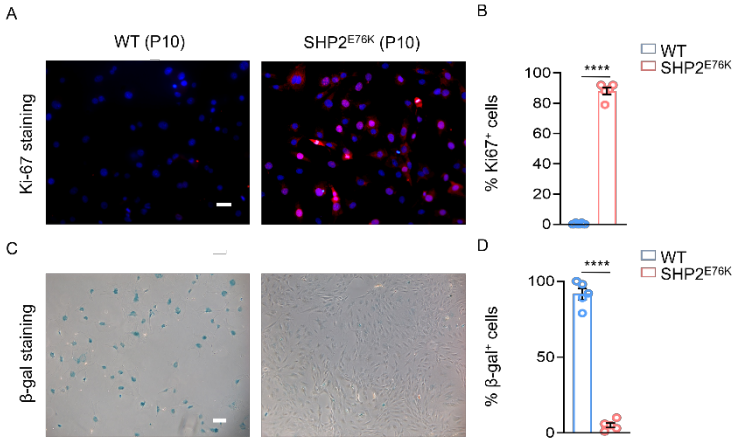

Supplemental Figure 5. The proliferation capacity of SHP2^{E76K} MSCs gradually accelerated, but WT MSCs progressively became senescent following successive passages. A, B Representative immunofluorescence images (**A**) and statistical analysis (**B**) of Ki67 staining in WT and mutant MSCs at the indicated passages (n=5 per group). Scale bar, 200 μm. Data are represented as the means ± SD. ****$p <$ 0.00001 (two-tailed unpaired t test). **C, D** Representative images (**C**) and statistical analysis (**D)** of β-gal staining in WT and mutant MSCs at the indicated passages (n=5 per group). Scale bar, 200 μm. Data are represented as the means ± SD. ****$p < 0.00001$ (two-tailed unpaired t test).

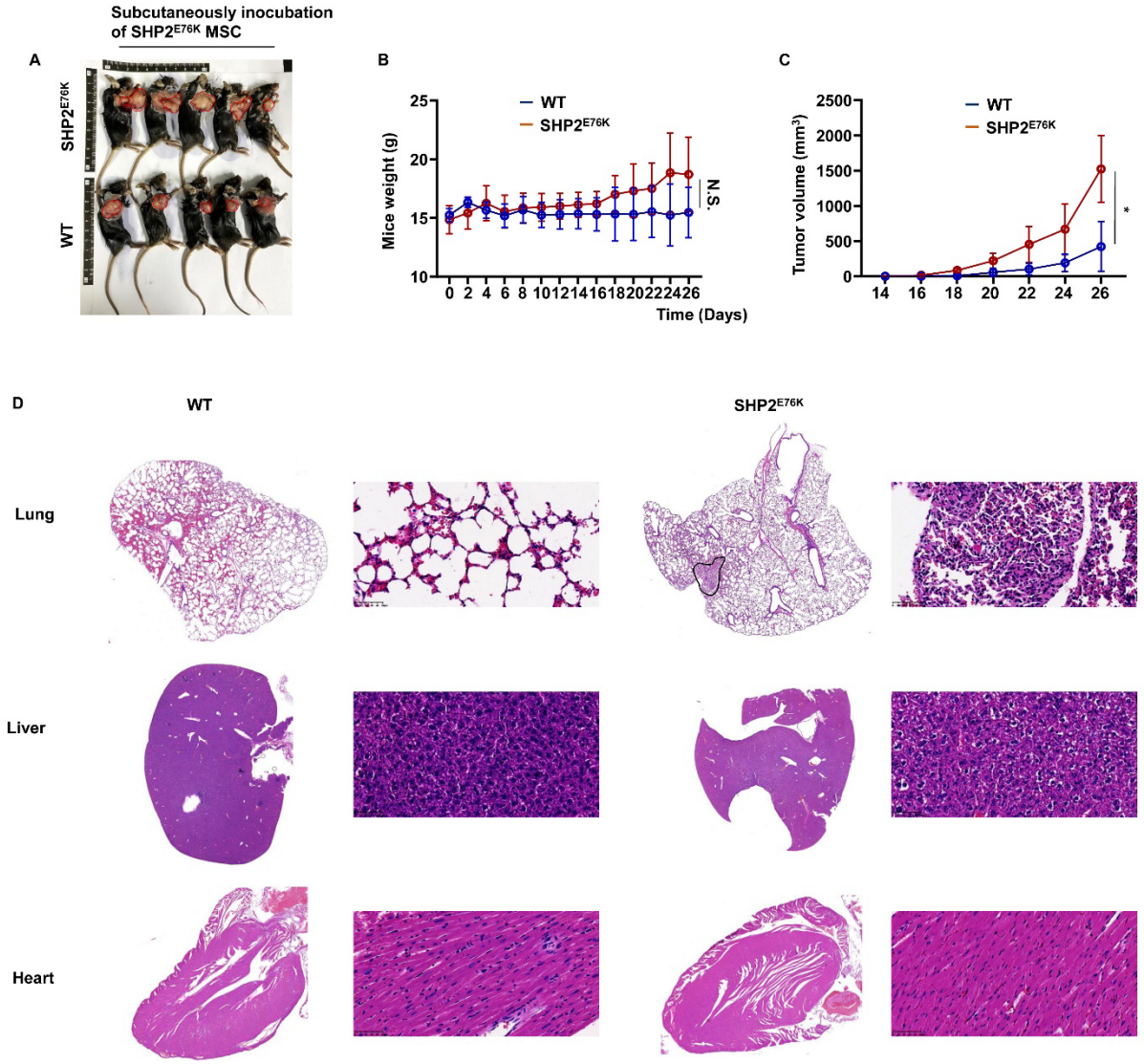

Supplemental Figure 6. SHP2^{E76K} MSCs can initiate sarcomagenesis and lung metastasis in C57BL/6 mice. A Representative image of tumors in WT and Mx1-cre; SHP2^{E76K} mice with SHP2^{E76K} MSCs inoculation. **B**, **C** Statistical analysis of mice wight (**B**) and tumor volume (**C**) of WT and Mx1-cre; SHP2^{E76K} mice (n=5 per group) with SHP2^{E76K} MSCs inoculation at different time points. Data are represented as the means ± SD. *$p < 0.05$, N.S. indicates no significance (two-tailed unpaired t test). **D** Representative HE staining images of Lung, liver and heart in C57BL/6 mice inoculated with WT or SHP2^{E76K} MSCs. Scale bar, 50 μm.

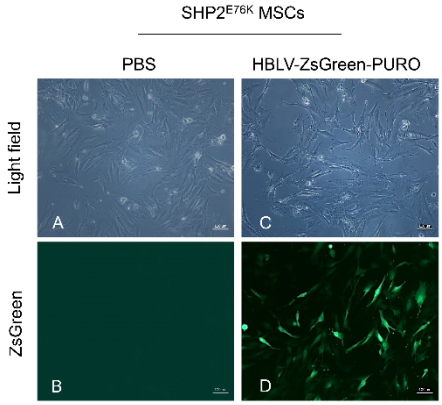

Supplemental Figure 7. Lentivirus transfection of ZsGreen in SHP2^{E76K} MSCs. A, B Representative light field images (**A**) and fluorescence images (**B**) of SHP2^{E76K} MSCs without lentivirus transfection. **C, D** Representative light field images (**C**) and fluorescence images (**D**) of SHP2^{E76K} MSCs overexpressing ZsGreen. Scale bar, 100 μm.

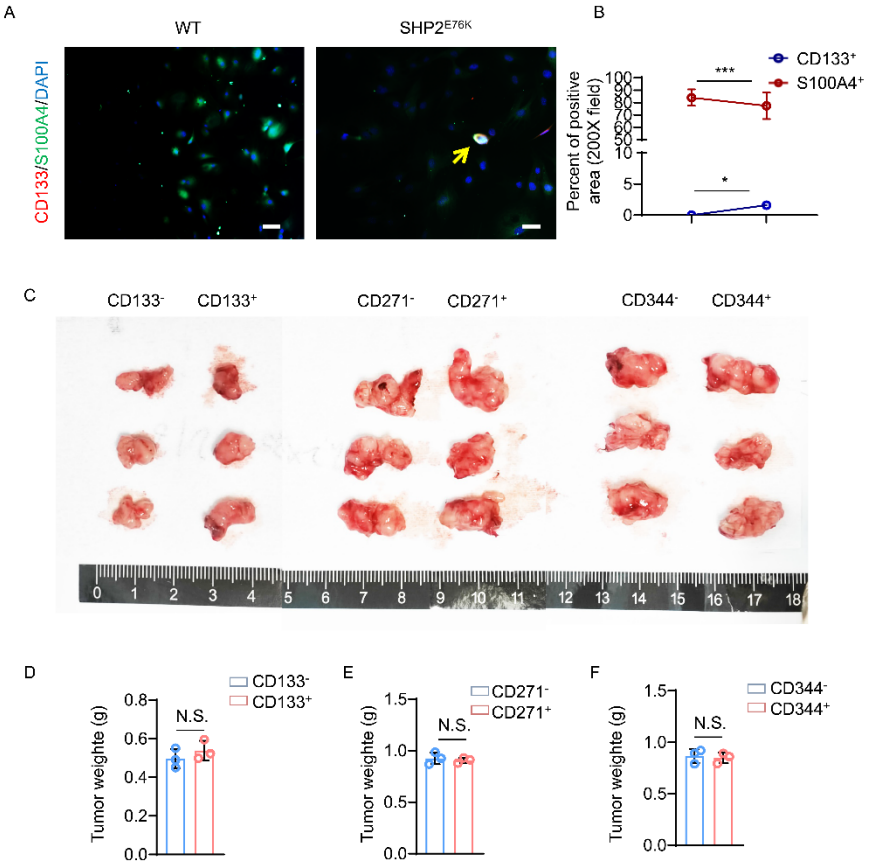

Supplemental Figure 8 CD133, CD271 and CD344 positive cells did not exhibit difference in tumor progression among SHP2^{E76K} MSCs. A, B Representative IF staining images (**A**) and statistical analysis (**B**) of S100A4 and CD133 in WT and SHP2^{E76K} MSCs. Scale bar, 200 μm. Data are represented as the mean ± SD. *$p < 0.05$, ***$p < 0.001$ (two–tailed unpaired *t* test). **C-F** Representative tumor images and statistical analysis of tumor developed by CD133$^-$, CD133$^+$, CD271$^-$, CD271$^+$, CD344$^-$ and CD344$^+$ SHP2^{E76K} MSCs (n=3 per group).

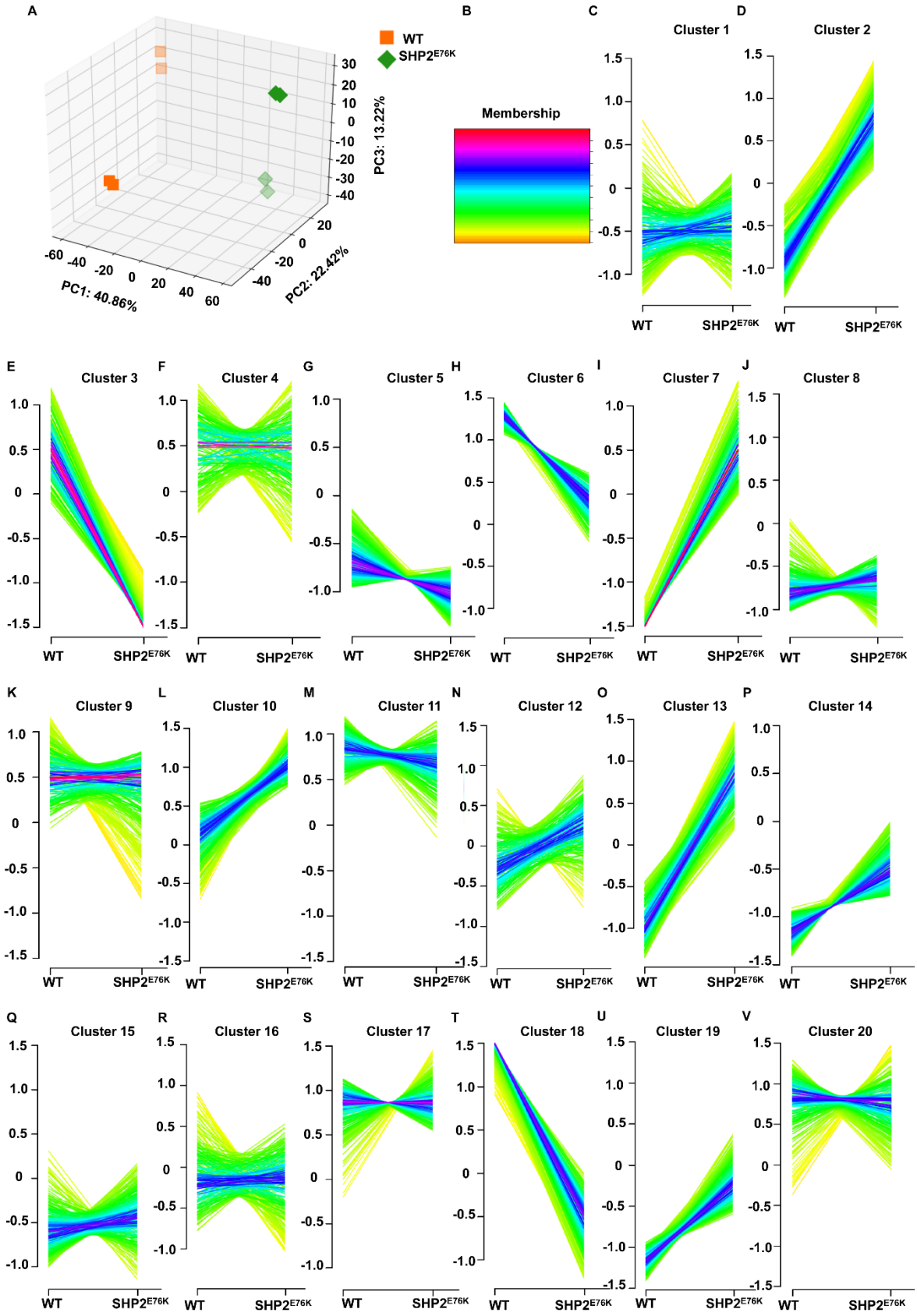

Supplemental Figure 9 PCA and trend analysis of WT and SHP2^{E76K} MSCs. A PCA of the WT and SHP2^{E76K} MSCs. **B-V** Trend analysis of WT and SHP2^{E76K} MSCs.

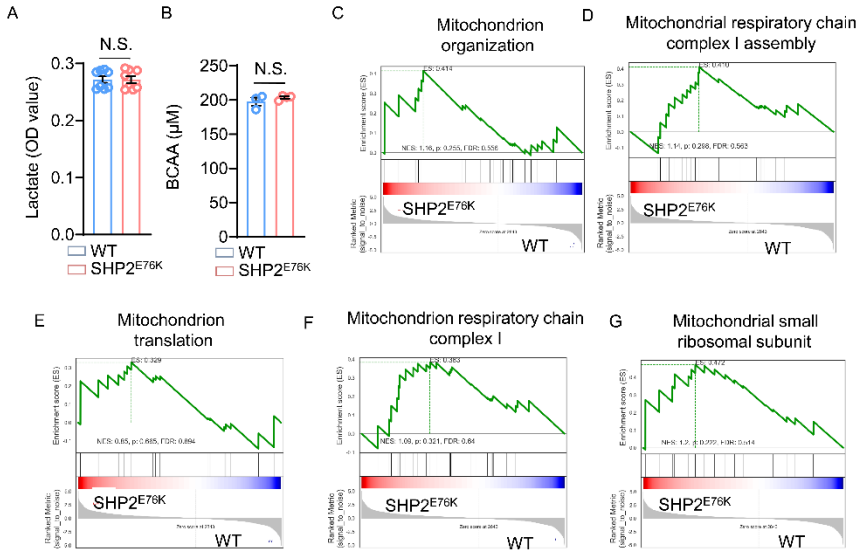

Supplemental Figure 10. Some metabolic parameters of SHP2^{E76K} MSCs did not change significantly, but mitochondria-associated proteins were enriched in SHP2^{E76K} MSCs. A Statistical analysis of the content of lactate in WT and SHP2^{E76K} MSCs (n=8 per group). Data are represented as the means ± SD. N.S. indicates no significance (two-tailed unpaired *t* test). **B** Statistical analysis of the content of BCCA in WT and SHP2^{E76K} MSCs (n=3 per group). Data are represented as the means ± SD. N.S. indicates no significance (two-tailed unpaired *t* test). **C-G** GSEA of mitochondria-associated proteins in WT and SHP2^{E76K} MSCs.

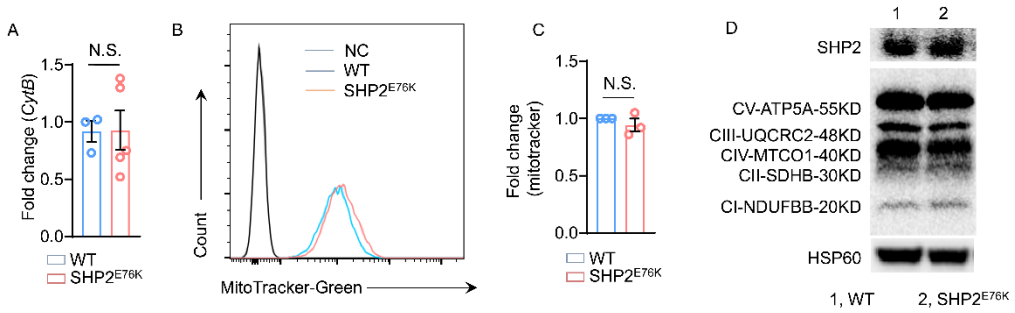

Supplemental Figure 11. Mitochondrial biogenesis, gene expression and complex expression in SHP2^{E76K} MSCs did not change significantly. A Statistical analysis of *CytB* expression in WT and SHP2^{E76K} MSCs (n=3 or 5 per group). Data are represented as the means ± SD. N.S. indicates no significance (two-tailed unpaired *t* test). **B, C** Representative image of flow cytometry (**B**) and statistical analysis (**C**) of MitoTracker Green staining in WT and SHP2^{E76K} MSCs using flow cytometry (n=3 per group). Data are represented as the means ± SD. N.S. indicates no significance (two-tailed unpaired *t* test). **D** Western blot analysis of the expression of mitochondrial complex-associated proteins in WT and SHP2^{E76K} MSCs.

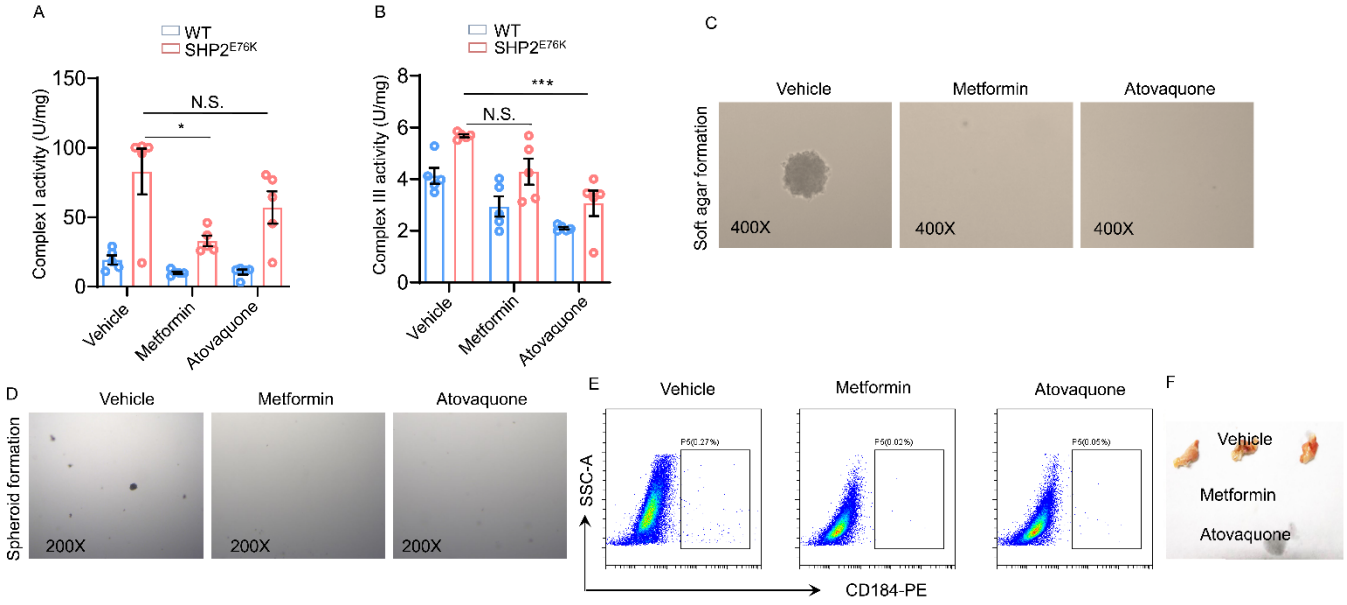

Supplemental Figure 12. Metformin and atovaquone effectively inhibited the complex I and III activity and the population of CD184^{+} cells in SHP2^{E76K} MSCs. A, B Statistical analysis of the activity of complexes I (**A**) and III (**B**) in WT and SHP2^{E76K} MSCs following metformin and atovaquone treatment (n=5 per group). Data are represented as the means ± SD. *$p < 0.05$, ***$p < 0.001$, N.S. indicates no significance (Two-way ANOVA with multiple-comparison test). **C**, **D** Representative images of soft agar formation and spheroid formation of SHP2^{E76K} MSCs with or without metformin and atovaquone treatment at indicated field. **E**, **F** Representative flow cytometry analysis of the population of CD184^{+} cells and tumor formation of SHP2^{E76K} MSCs with or without metformin and atovaquone treatment.

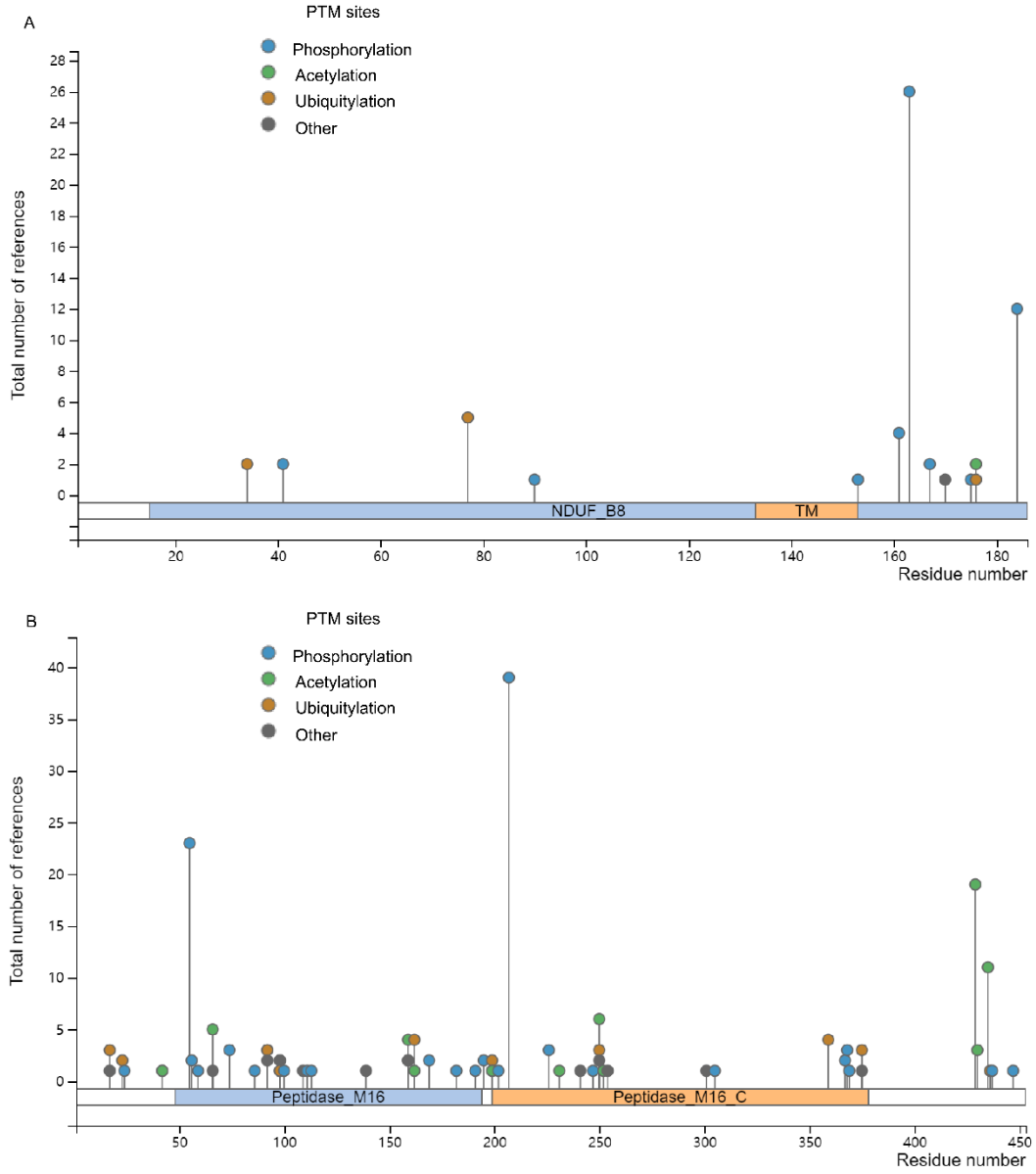

Supplemental Figure 13. Protein posttranslational modification sites of NDUFB8 and UQCRC2. A Protein posttranslational modification sites of NDUFB8, including phosphorylation, acetylation and ubiquitylation sites. **B** Protein posttranslational modification sites of UQCRC2, including phosphorylation, acetylation and ubiquitylation sites. Data are extracted from https://www.phosphosite.org.

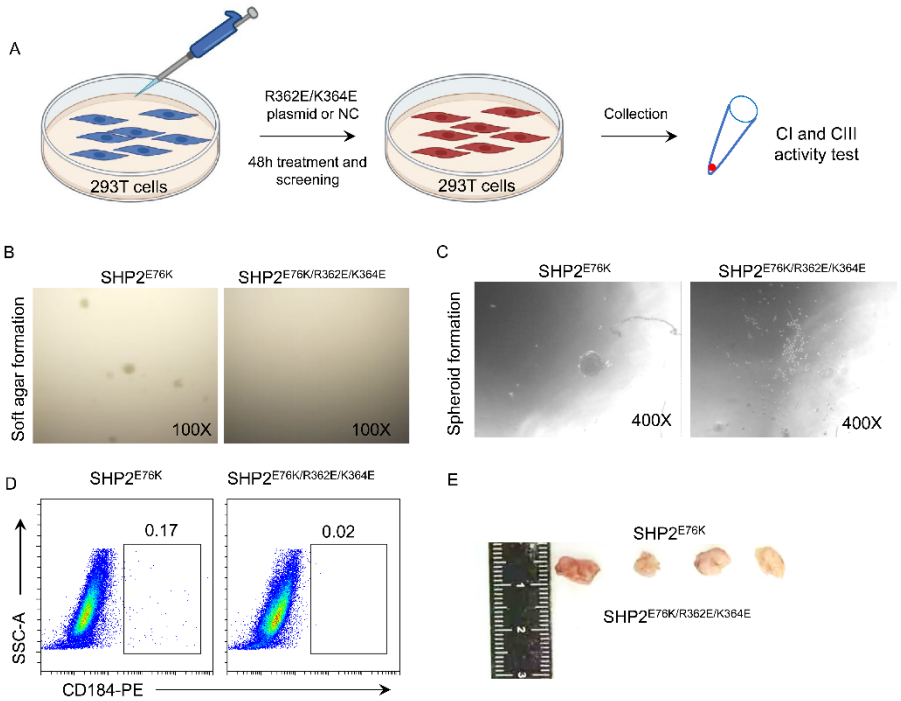

Supplemental Figure 14. SHP2 LLPS-defective mutation rescues the malignancy of SHP2^{E76K} MSCs. **A** The Working flow that infection of SHP2 LLPS-defective mutation in 293T cells. **B, C** Representative soft agar images (**B**) and tumor spheroid formation (**C**) of SHP2^{E76K} MSCs with or without R362E/K364E infection. **D, E** Representative flow cytometry analysis of CD184^{+} cells (**D**) and tumor formation (**E**) of SHP2^{E76K} MSCs infected with R362E/K364E plasmid.

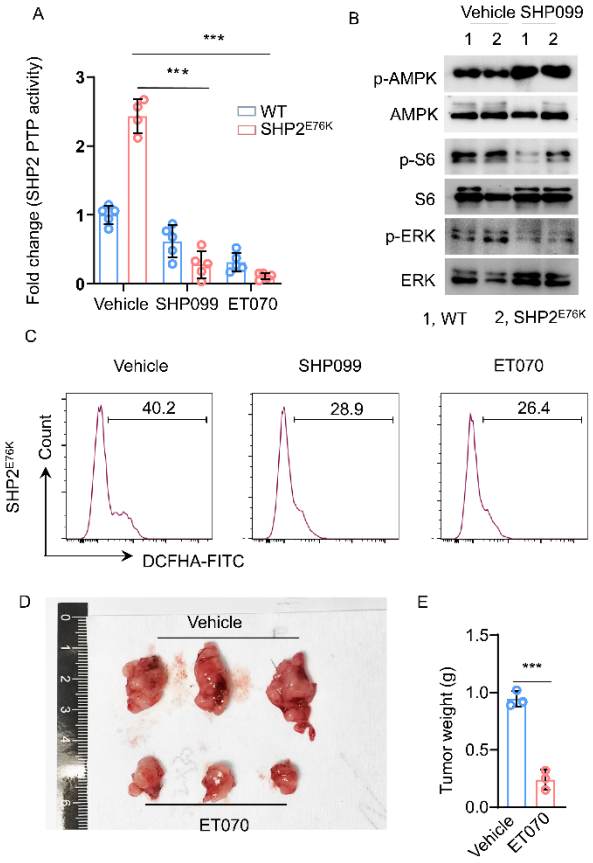

Supplemental Figure 15. Alteration of SHP2 activity, downstream molecules and associated malignant cell behavior in SHP2^{E76K} MSCs following treatment with SHP2 inhibitors. A Statistical analysis of SHP2 activity in WT and SHP2^{E76K} MSCs treated with SHP099 and ET070 (n= 5 per group). Data are represented as the means ± SD. $^{**}p < 0.01$ (Two-way ANOVA with multiple-comparison test). **B** Representative western blot images of the AMPK and ERK pathways in WT and SHP2^{E76K} MSCs treated with SHP099 or ET070. **C** Representative flow cytometry images of ROS levels of SHP2^{E76K} MSCs treated with SHP099 or ET070. Images were captured at a 200X field. **D**, **E** Representative tumor images (**D**) and statistical analysis (**E**) of tumor developed by SHP2^{E76K} MSCs treated with ET070 (n=3 per group). Data are represented as the means ± SD. $^{***}p < 0.001$ (two-tailed unpaired t test).